ISSN: 2458-8989

Natural and Engineering Sciences

NESciences, 2026, 11 (2): 124-139 doi: 10.28978/nesciences.262011

Polymer-Based Dune Stabilization for a Climate-Resilient Control of Active Desertification

Mohammed Mahdi Al-Mossawi[1*], Muqdad T. Sedkhan[2], Meelad A. Hussein[3], Lamees S. Al-Qurnawy[1], Hala A. Shabar[1], Wisam R. Muttashar[1], Maher M. Mahdi[2], and Salah M. Al-Atab[4]

[1] Marine Science Centre, University of Basrah, Basrah, 61004, Iraq.

[2] Department of Geology, Science College, University of Basrah, Basrah, 61004, Iraq.

[3] College of Marine Science, University of Basrah, Basrah, 61004, Iraq.

[4] Department of Soil Science and Water Resources, College of Agriculture, University of Basrah, Basrah, 61004, Iraq.

Abstract

Desertification driven by active dune soils poses a major environmental challenge in arid regions and is increasingly intensified by climate variability. In southern Iraq, migrating dunes frequently encroach on major highways, creating dangerous driving conditions and imposing high maintenance costs, which underscores the urgent need for effective and practical stabilization solutions. This study aims to evaluate the effectiveness of carboxymethyl cellulose (CMC), a cellulose-based polymer, for stabilizing dune soils collected from five representative sites along active dune fields in southern Iraq. Dune soil samples were treated with CMC concentrations ranging from 10% to 50% and tested over curing periods of up to 80 days. The experimental program was supported by chemical, mineralogical, and penetration resistance analyses, and by multivariable regression modeling to quantify the joint effects of polymer content and curing time. The results demonstrate a substantial improvement in soil strength following CMC treatment. At 10% CMC content, penetration resistance increased by approximately 140–165% after 28 days of curing compared with untreated soil, while higher polymer dosages (40–50%) produced strength increases exceeding 300% relative to natural dune soil. The most pronounced gains occurred within the first 28 days, after which penetration resistance values stabilized, indicating completion of the curing and bonding process. These findings demonstrate that CMC significantly enhances the mechanical resistance of dune soils and offers an environmentally compatible solution for limiting dune migration in desertification-prone regions, particularly in areas adjacent to infrastructure where improved soil stability is required.

Keywords:
Desertification control, Dune stabilization, Polymer treatment, carboxymethyl cellulose (CMC), Climate-Resilient.

Available online: 02/06/2026

1 Introduction

Desertification threatens sustainable development and undermines land productivity, aggravating water scarcity, biodiversity loss, and climate vulnerability (UNCCD, 2019 & 2018; IPCC, 2019). Desertification

*Corresponding Author: Mohammed Mahdi Al-Mossawi, E-mail: mohammed.mahdi@uobasrah.edu.iq

is a major environmental challenge in arid and semi-arid regions and is increasingly intensified by climate variability. Drylands globally cover about 46.2% of Earth's land area and are home to about 3 billion people (IPCC, 2019). In Iraq, one of the countries most susceptible to global climate impact (Iraq I.O.M, 2022), the problem is expressed prominently through active dune migration and wind-driven sand encroachment that disrupts transportation corridors and built infrastructure, especially highways crossing desert margins. The study area along the Nasiriya–Baghdad highway (Thi Qar and surrounding provinces) exemplifies this issue, where dune sediments repeatedly accumulate on roads and create hazardous driving conditions (Yahia et al., 2023), which requires appropriate approaches to treat or mitigate these desertification hazards. Traditional methods for stabilizing dunes and sand have relied on mineral binders and industrial byproducts, such as silicate-based materials and cement-related compounds (Sujatha & Kannan, 2022a). The researchers tested silica gel and cement kiln dust as stabilizers for dune sands, finding significant improvements in shear strength and California Bearing Ratio (CBR) values after 28-day curing periods (Rammal & Jubair, 2015).

More recently, polymer and biopolymer stabilizers have gained attention for their rapid particle binding through electrostatic and hydrogen bonding mechanisms (Chang et al., 2020); ability to form protective surface crusts that resist wind shear (Chen et al., 2019); capacity to substantially reduce wind erosion rates in wind-tunnel tests (Mirzaei et al., 2021); and enhancement of soil moisture retention via hydrophilic polymer chains (Soldo et al., 2020). Cellulose-derived polymers, especially sodium carboxymethyl cellulose (NaCMC/CMC), are increasingly studied as sustainable soil additives due to their binding ability and hydrophilicity (Sujatha & Kannan, 2022b). For example, NaCMC has been reported to significantly increase the unconfined compressive strength and reduce hydraulic conductivity of fine-grained soils (Abdelgelil et al., 2025b), with microstructural observations linking this performance to viscous/fibrous polymer binding networks rather than the formation of new mineral phases (Abdelgelil et al., 2025a). Recent experimental work on cellulose-ether ecological sand-fixing materials, including CMC-based systems, has shown that treated sands develop strong sand-fixing crusts and markedly improved wind-erosion resistance with curing time, supporting the concept that polymer-bound crusts strengthen with ageing (Zhang et al., 2024). Most previously studied additives, including blends of polymeric materials such as urea-formaldehyde or bentonite, are generally regarded as either cost-effective but potentially environmentally unfriendly, or difficult to prepare. Hence, a polymeric material with high viscosity was prepared and tested in the current study, serving as an effective soil stabilizer and being both environmentally friendly and cost-effective. This is very important for materials designed to address environmental problems.

Yahia et al. (2023) studied dune soil improvement in southern Iraq using carboxymethyl cellulose (CMC) resin, which was less cost-effective and environmentally friendly. They compared natural dune soil mixed with polymer (PNS) to natural soil mixed with polymer at a fixed water content (POM). The work provided important initial evidence that CMC can enhance the mechanical behavior of dune soils, where this study developed. However, the study remained limited by (i) small spatial coverage (one-site emphasis), (ii) incomplete mineralogical characterization, and (iii) limited ability to generalize treatment performance across variable dune compositions and site conditions.

Therefore, the current study aims to evaluate carboxymethyl cellulose (CMC) polymer resin as a dune soil stabilizer using multiple sampling sites along the southern Iraq dune regions. Soil was sampled and treated under controlled polymer concentrations (10–50%) and moisture conditions, and assessed through a chemical, mineralogical, and penetration resistance testing, and then statistical/regression modeling relating resistance to curing time and polymer content. This predictive model of polymer-treated dune soil offers a practical tool for engineering and agricultural applications and supports preliminary design and decision-making in desertification mitigation efforts.

1.1 Theoretical Background:

Polymer-based stabilization has been increasingly adopted as a practical and environmentally compatible alternative. Unlike traditional mineral stabilizers, such as cement or lime, polymers enhance soil behavior and strength improvement primarily through physical and physicochemical interactions rather than through mineralogical cementation (Garcia et al., 2015; Mohammadian et al., 2024), where the polymer addition produces more stable soil fabric by increasing interparticle bonding and aggregation. Cellulose-derived polymers, particularly carboxymethyl cellulose (CMC), have been shown to exhibit hydrophilicity, high viscosity, and effective particle-binding behavior, leading to improved mechanical and hydraulic soil properties through physical bonding mechanisms (Sujatha & Kannan, 2022b). CMC is characterized by high molecular weight and strong hydrophilicity, enabling it to absorb water and form viscous gel-like

structures within the soil pore space. When mixed with sandy or silty soils, CMC chains adsorb onto mineral surfaces and bind adjacent particles through hydrogen bonding, electrostatic attraction, and cation bridging, particularly in soils rich in calcium and sodium ions (Amézketa, 1999; Abdelgelil et al., 2025a). Experimental evidence from southern Iraq supports the effectiveness of CMC in stabilizing dune soils. Yahia et al. (2023) reported that adding CMC to dune soils resulted in measurable improvements in mechanical behavior, particularly in terms of shear strength. Their results showed that both Polymer–Natural Soil (PNS) and Polymer–Optimum Moisture (POM) mixtures-maintained friction-dominated behavior typical of sandy silt soils but exhibited increased friction angles at low polymer dosages. Micro-scale observations revealed the formation of filamentous CMC structures within the soil matrix, which promoted particle aggregation and enhanced resistance to shear deformation. The CMC forms filamentous and gel-like structures within the soil matrix as shown in Figure 1, reducing evaporation and maintaining favorable moisture conditions during curing. Preliminary observations confirm that both PNS and POM mixtures exhibit enhanced moisture preservation relative to untreated (natural) soil.

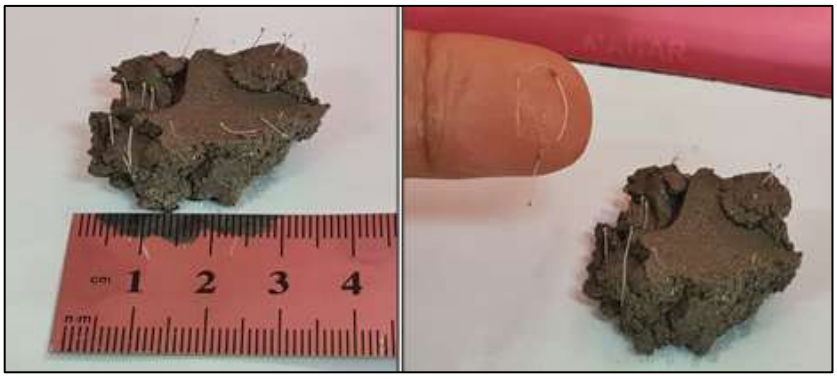

Figure 1 Polymer growth observed after 14 days of placement on the soil mixture.

Regarding the time factor, the soil strength gains increase with curing time and approach a stable condition once polymer bonding and moisture equilibrium are achieved (Yuan et al., 2020; Zhang et al., 2024). The formation of polymer networks, redistribution of moisture, and progressive physical hardening occur gradually, resulting in time-dependent increases in soil resistance. These emphasizes the importance of incorporating curing time as a governing variable in evaluating stabilized dune soils.

Overall, it is believed that CMC stabilization improves dune soil performance through combined effects of particle binding, moisture retention, and curing-time-dependent hardening. Building upon the findings of Yahia et al. (2023), the present study extends this understanding by examining multiple sampling locations, a wider range of polymer contents, penetration resistance behavior, and regression-based performance modeling, thereby providing a more comprehensive assessment of CMC-treated dune sediments.

2 Methods and Materials

2.1 Site Description

The study area is located in southern Iraq, spanning three provinces, northwest of Thi-Qar, northeast of Al Muthanna, and south of Al Qadisiya. This dune sediment region is part of the desert zone, extending eastward from the Tigris River, the north side of the Euphrates River, and the Al-Gharraf River (Yahia et al 2023). Figure 1 shows the location of the study area, including the types of sediments present and the five sampling stations.

Geologically, the study area is located within the southern part of the Mesopotamian Basin featured by thick accumulations of Quaternary deposits. The region is dominated by Holocene to Late Pleistocene sediments, including extensive aeolian deposits, floodplain alluvium, and dry marsh deposits (Sissakian, Al Ansari, & Adamo, 2021), as shown in Figure 2. The aeolian sediments form widespread active and semi-active dune fields, reflecting prolonged arid to hyper-arid climatic conditions and abundant unconsolidated sediment supply (Othman et al., 2019). These dune sands are predominantly fine- to medium-grained, well sorted, and weakly cemented, and then highly susceptible to wind erosion and migration. The alluvial units are associated mainly with the Euphrates River and its distributaries, particularly the Shatt Al-Gharraf system from the east, Figure 2, which supplies and reworks sediments across the basin (Colip et al.,2025).

The movement of dune soil across highways has caused many tragic accidents and posed major problems for infrastructure, including roads, airports, and factories. This natural hazard usually occurs for several months each year, starting at the end of spring and continuing into mid-summer Figure 3.

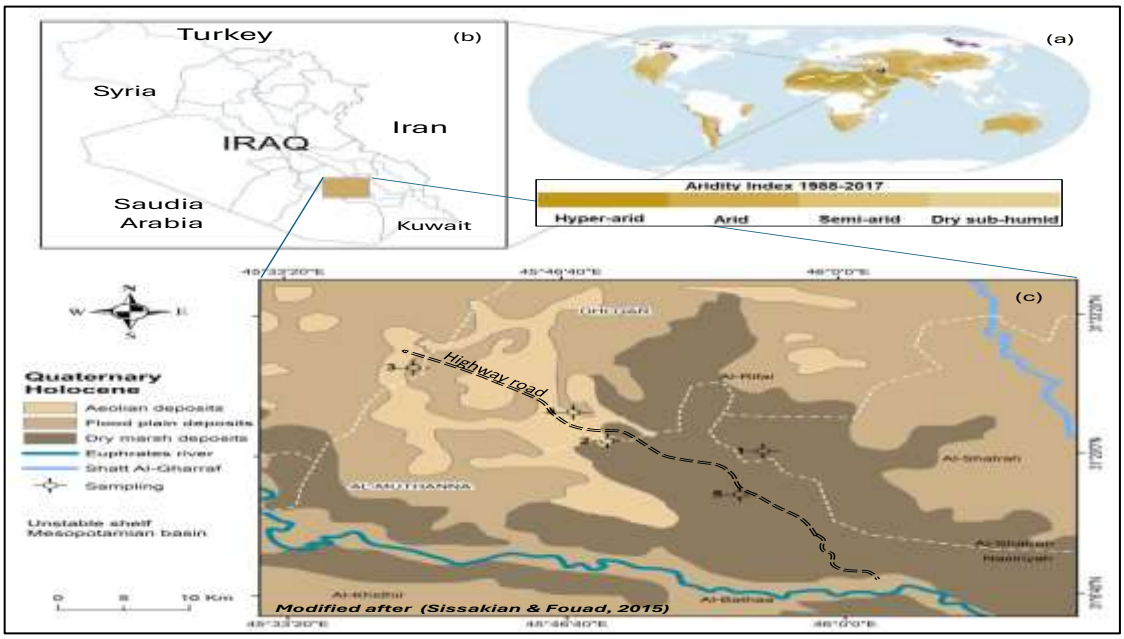

Figure 2 Composite location map of the study area in southern Iraq showing (a) the regional aridity classification, (b) the geographical location within Iraq, (c) the geological setting of the southern Mesopotamian Plain, and (d) the distribution of the five dune soil sampling stations along active dune fields adjacent to major highway corridors.

Figure 3 landform of dune sediment, where the samples were collected.

2.2 Preparation of soil and polymer materials

2.2.1 Preparation of Polymer Solution

Carboxymethyl cellulose (CMC) solutions were prepared by dissolving 10, 20, 30, 40, and 50 g of CMC in 1000 mL of distilled water under continuous stirring. The mixture was heated to 50–60 °C to enhance

dissolution. The CMC powder was gradually added to the vortex to ensure uniform dispersion. Stirring and gentle heating were continued for 30–60 minutes until a homogeneous solution with full viscosity was achieved.

2.2.2 Preparation for Soil Samples

Soil samples were collected from the Basra governorate/region and taken from the surface layer (0-30 cm). The samples were air-dried, ground, and then sieved through a 1 mm mesh. Finally, soil particles smaller than 1 mm in diameter were stored in airtight glass containers until use.

2.2.3 Treating soil with a prepared polymer

20 mL of the prepared polymer was added to 500 g of soil with a moisture content of 17% (representing the field soil capacity). The soil was thoroughly mixed with the polymer solution and then dried at room temperature for the necessary measurements.

2.3 Sampling:

Dune soil samples were collected from five representative sites within the southern Iraqi dune sediment zone, as shown in Figure 1. The selected sites were chosen alongside nearly the highway road affected by the dune soils. The collected samples were placed in sealed containers, labeled, and transported to the laboratory for further preparation and testing.

2.4 Classification tests:

The soil type was determined by conducting grain size distribution analyses and evaluating consistency limits. Hydrometer and Atterberg limits tests were performed in accordance with ASTM standards. Additionally, standard Proctor tests were utilized to estimate the optimum moisture content and maximum dry density. The objective of these determinations was to facilitate the subsequent stage of mixture preparation.

2.5 Mixing procedure:

Two main groups of samples were experimentally designed. They are noted as Polymer-Natural Soil (PNS) and Polymer-Optimum-Moistured soi (POM). Each group includes five specimens that have different levels of polymer. The PNS group of specimens has five percentage levels of Polymer additions, including 10%, 20%, 20%, 40%, and 50% with no water. At the same time, the second POM group has the same five levels of Polymer (P) additions (10%, 20%, 30%, 40%, and 50%) yet with 17.5% of water (measured Optimum moisture content). The objective of this approach is to examine the soil's penetration resistance characteristics likely to be encountered under real field conditions. Using the assigned 17.5% of water with polymer addition in the POM group is based on the studied soil's optimum moisture content.

2.6 Soil Penetration Resistance

Pocket Pentrometer C-50 with graduations (0.5-5) was used. The pentrometer was placed on the surface of the soil sample to be tested and pressed until it penetrated the soil's surface layer. Then, withdraw the device from the soil and record its reading in kg/cm^2, then convert to kN/m^2.

2.7 Mineralogical analysis

The identification of heavy and light minerals of the five sites provides essential context for interpreting both the mechanical behaviour of the dune sediments and the performance of CMC treatment. Microscopic analysis was performed on the samples to identify the mineral structures and their concentrations, utilizing x-ray diffraction for sites 1, 2, and 3. Furthermore, both light and heavy minerals were analyzed and discussed. For the light minerals analysis, X-ray diffraction was used to analyze and identify the light minerals such as quartz and feldspar.

For the heavy minerals (minerals with a density greater than 2.9 g/cm^3), they are typically referred to as the denser components found in siliciclastic sediments, such as zircon, tourmaline, opaque minerals, pyroxene, epidote, chlorite, and biotite. A heavy mineral suite refers to the relative percentages of heavy minerals present in a rock. Since heavy minerals are a minor component of most sedimentary rocks, they must be isolated for detailed study. The separation of heavy minerals is commonly achieved using a dense liquid in a separatory funnel, with bromoform being a commonly used liquid.

2.8 Regression Analysis and Statistical Modeling

The combined effects of curing time and polymer content on soil resistance were quantified through multivariable linear regression models. Separate models were established for soils treated with PNS and

POM at each investigated site (Sites 1, 2, and 3). For each site, the resultant experimental data consisted of five curing periods (1, 7, 14, 21, and 28 days) and five polymer contents (10%, 20%, 30%, 40%, and 50%), yielding 25 observations per site. The model performance was evaluated using the coefficient of determination (R^2), root mean square error (RMSE) and mean absolute error (MAE) to assess fitness and prediction accuracy. The models were applied within the experimental ranges of curing time (1–28 days) and polymer content (10–50%).

3 Results

3.1 Baseline Properties of Untreated Dune Soils

3.1.1 Chemical analysis results:

Table 1 shows the chemical properties of the studied soil samples, indicating a moderately saline and alkaline soil environment. The relatively high levels of Ca^{2+} (6 meq/L) and Mg^{2+} (3.1 meq/L) suggest that divalent cations are predominant. These cations enhance soil aggregation by promoting electrostatic bridging between the negatively charged polymer chains (CMC) and soil particles. In addition, the high Na^{+} content (9 meq/L) reflects sodicity effects that generally weaken soil structure due to particle dispersion (Amézketa, 1999).

Table 1 The chemical properties of the untreated (natural) dune soils of the study area.

Mg^{+2} Meq/l	**Ca^{+2} Meq/l**	**K^{+} Meq/l**	**Na^{+1} Meq/l**	**CO_3^{-2} Meq/l**	**HCO_{-3} Meq/l**	**SO_4^{-2} Meq/l**	**CL^{-} Meq/l**	**$CaSO_4$ gkg-1**	**$CaCO_3$ gkg-1**	**EC mls/cm**	**PH**
3.1	6	1.1	9	0	2.9	5.6	6.5	429.27	205.72	3.50	7.51

3.1.2 Physical properties of studied dune soils:

Table 2 presents the physical properties of the untreated (natural) dune soils in the study area, showing a high total porosity (52.08%) and a low bulk density (1.27 g/cm³). This indicates a loose soil structure with significant voids, which typically reflects low penetration resistance.

In addition, the low plasticity index (PI = 7.8) classifies the soil as low-plastic, making the soil highly responsive to polymer treatment, as polymers can significantly improve interparticle bonding where natural cohesion is limited.

Table 2: The physical properties of the untreated (natural) dune soils of the study area.

Total Porosity (%)	**Specific gravity, Gs (g/cm^3)**	**Bulk density, r_b (g/cm^3)**	**Plasticity index (P.I.)**	**Plastic limit (P.L)**	**Liquid limit (L.L)**	**Fine content (%)**	**Sand (%)**	**Optimum Moisture Content, (%)**	**Max. Dry Density, g_d (kN/m^3)**
52.08	2.65	1.27	7.8	24.21	32.01	71	29	17.5	17.8

3.2 Effect of CMC Content and Curing Time on Penetration Resistance:

Results of penetration resistance illustrated the effect of the polymer materials CMC added to the natural sand soil PNS and to the moist soil POM, as well as the penetration resistance for natural soil NS as a control. Figures 3, 5, and 7 represent the outcomes of PNS, while figures 4, 6, and 8 represent the outcomes of POM for three chosen sites.

3.2.1 Site-1: penetration resistance of the polymer CMC added to the natural soil (PNS) and moist soils (POM)

As shown in Figure4, the soil penetration resistance of PNS with 10% polymer was 3.9, then increased to 10.1 kN/m²·10-7 after 28 days. Meanwhile, the 50% concentration reached 10.6 and 17.7 KN/m²·10-7 after 1 and 28 days, respectively. After 28 days, the values remained almost constant. Similarly, Figure 4 shows that the resistance of POM with 10% polymer rose from 4.5 to 11.3 kN/m²·10-7 after 28 days. The soil penetration resistance stayed steady at 11.6-11.5 kN/m²·10-7 after 56 and 84 days. Therefore, the correlation between the additive polymer and soil penetration resistance is stronger with CMC. Both figures 4 and 5 show a generally consistent pattern with a slight increase in resistance after 28 days of adding the polymer in natural and moist soil. This minor rise could be caused by water evaporation. The increase in

physical hardening is most likely due to the cohesion and binding effects of the polymers, which act as strong bonding agents, filling pore spaces and creating adhesive bonds between soil particles. Additionally, the results indicate that penetration resistance increased at all concentrations from 1 to 28 days, then plateaued. However, the soil penetration resistance for natural soil without polymer (control) did not change over time across different concentrations.

.

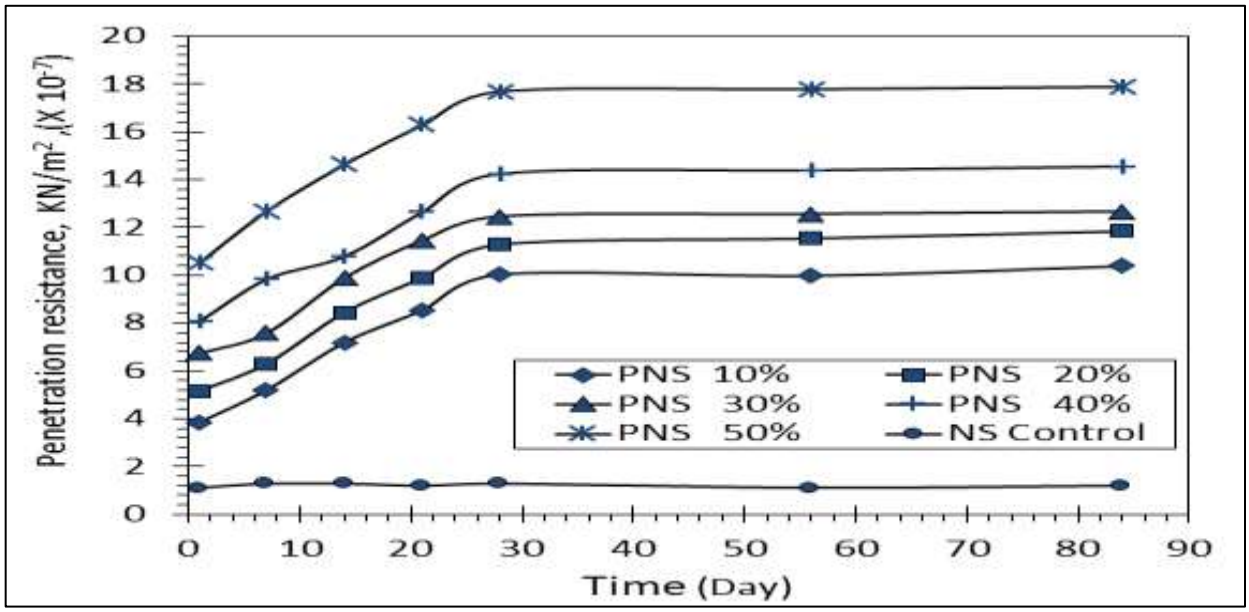

Figure 4 Soil penetration resistance of adding the polymer CMC with 5 concentrations (10, 20, 30, 40, and 50%) to the moist soil (PNS) in site 1 within 84 days.

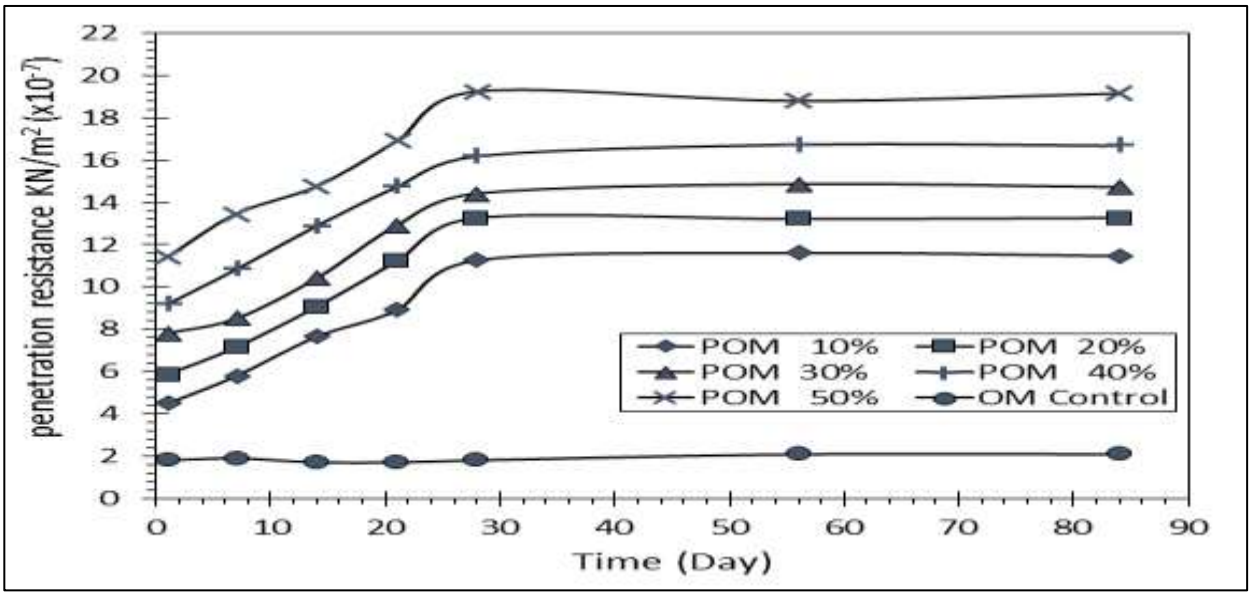

Figure 5 Soil penetration resistance of adding the polymer CMC with 5 concentrations (10, 20, 30, 40 and 50%) to the moist soil (POM) in site 1 within 84 days.

3.2.2 Site-2: penetration resistance of the polymer CMC added to the natural soil (PNS) and moist soils (POM)

A similar pattern to site 1, at site 2. The results show where resistance increases with the same additive levels (Figures 6 and 7). Soil penetration resistance with 10% polymer additive and natural soil PNS was 3.8 kN/m²·10-7, then rose to 9.8 kN/m²·10-7 after 28 days, while with 50% polymer it was 10.5 kN/m²·10-7 after 1 day and 17.6 kN/m²·10-7 after 28 days. Similarly, soil penetration resistance with 10% POM was 4.6 kN/m²·10-7 after 1 day and 11.2 kN/m²·10-7 after 28 days. For 50% polymer, resistance was 11.2 kN/m²·10-7 after 1 day and 19.3 kN/m²·10-7 after 28 days. The results show that soil penetration resistance

increases over time when mixed with polymers. The polymer additive POM shows greater penetration resistance as its concentration exceeds that of PNS over time.

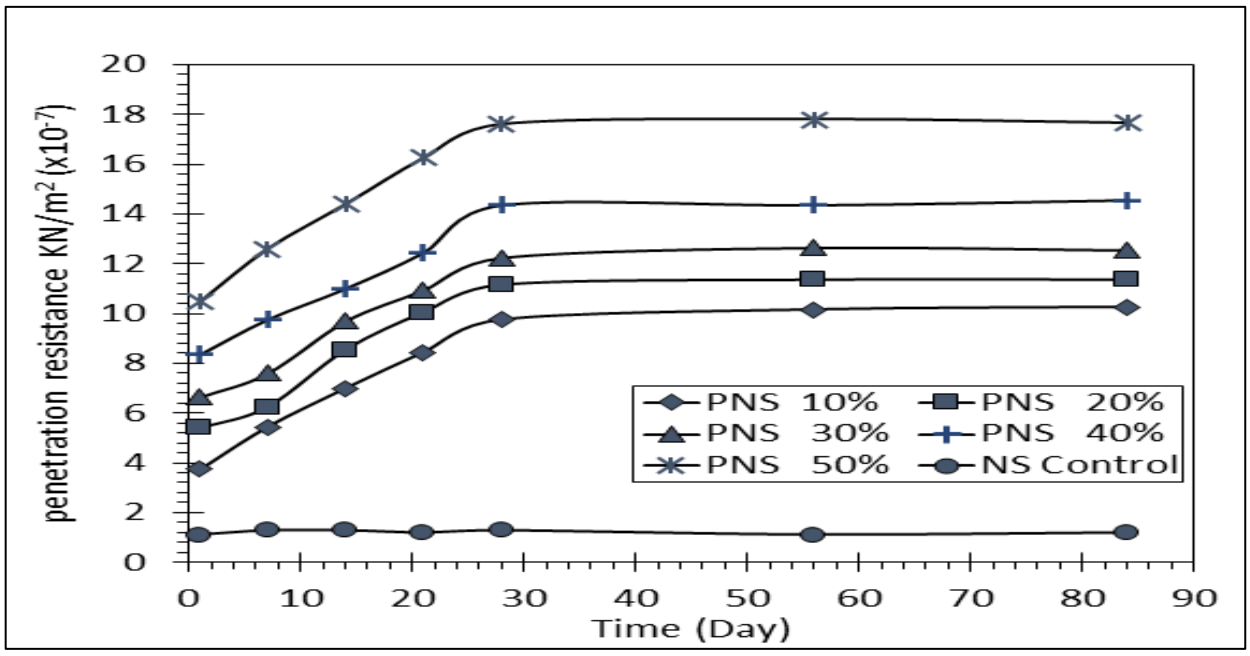

Figure 6 Soil penetration resistance of adding the polymer CMC with 5 concentrations (10, 20, 30, 40 and 50%) to the moist soil (PNS) in site 2 within 84 days.

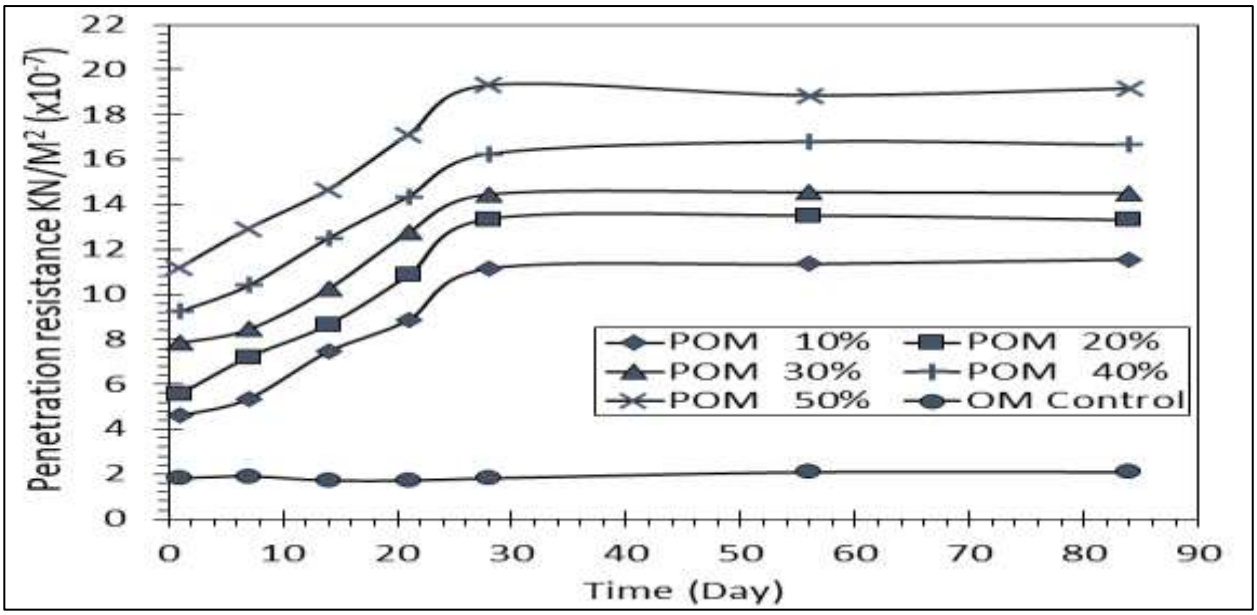

Figure 7 Soil penetration resistance of adding the polymer CMC with 5 concentrations (10, 20, 30, 40 and 50%) to the moist soil (POM) in site 2 within 84 days.

3.2.3 Site-3: penetration resistance of the polymer CMC added to the natural soil (PNS) and moist soils (POM)

Figures 8 and 9 show a generally consistent pattern that is similar to those at sites 1 & 2. Soil penetration resistance also increases in both soils, PNS and POM. The results demonstrate a steady increase in penetration resistance with increasing polymer content from 10% to 50% in PNS, which is lower than the increase observed at the same concentrations in POM over time.

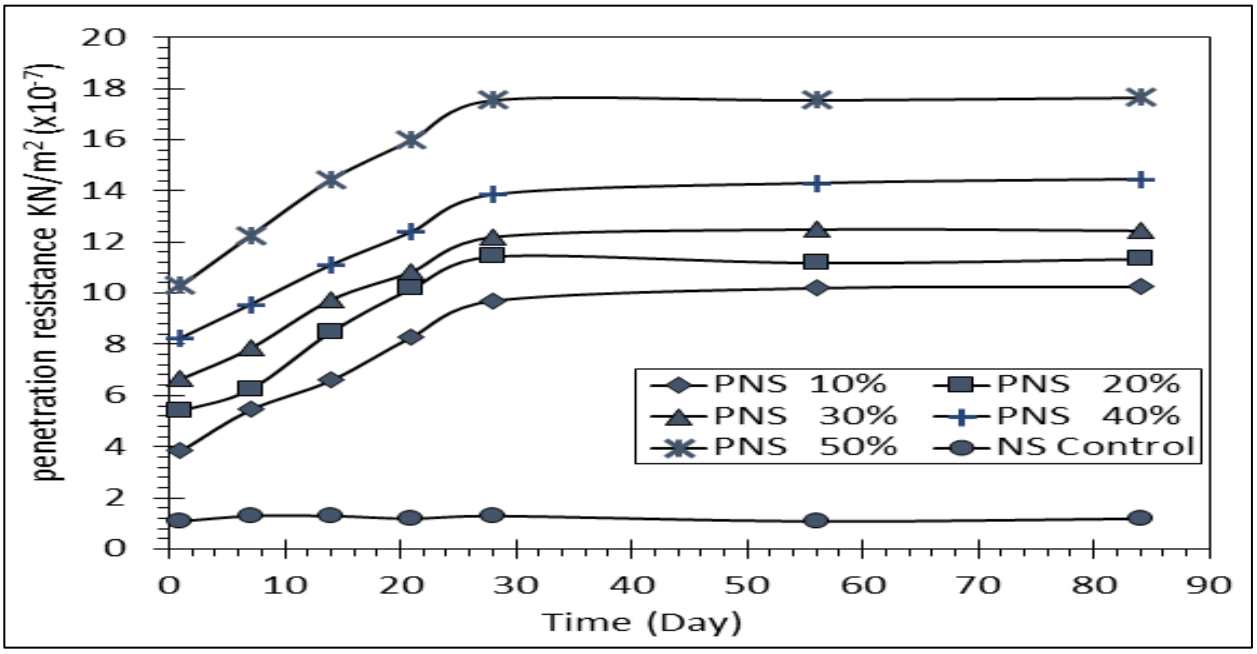

Figure 8 Soil penetration resistance of adding the polymer CMC with 5 concentrations (10, 20, 30, 40 and 50%) to the moist soil (PNS) in site 3 within 84 days.

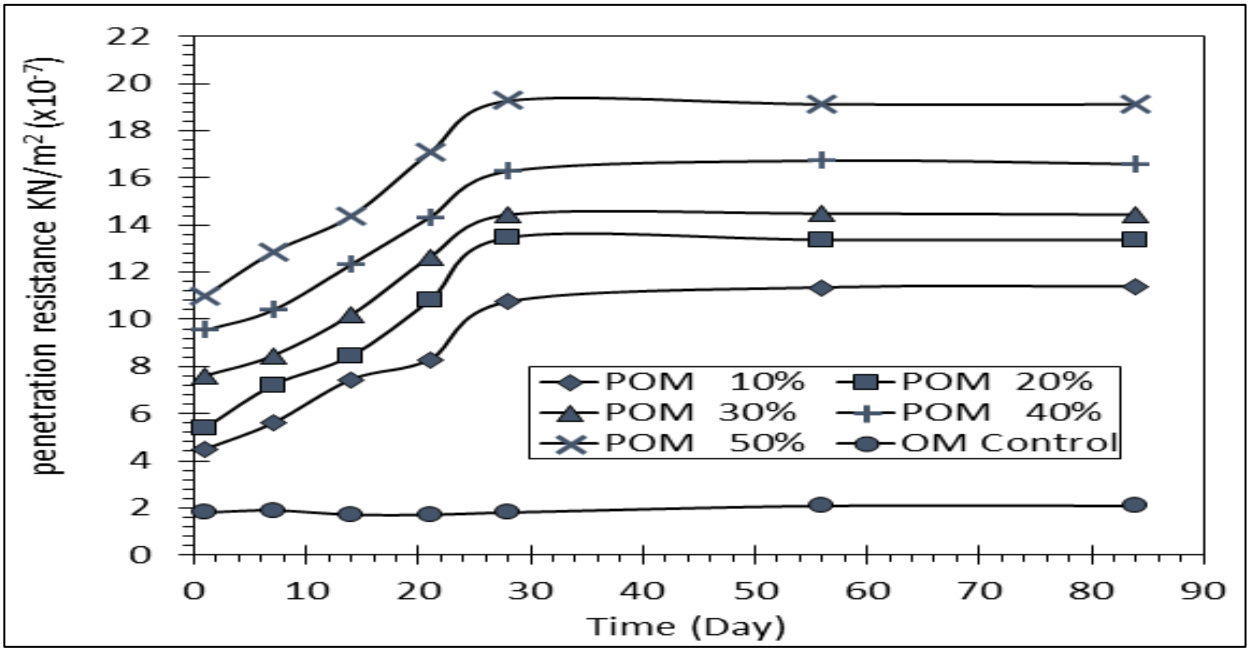

Figure 9 Soil penetration resistance of adding the polymer CMC with 5 concentrations (10, 20, 30, 40 and 50%) to the moist soil (POM) in site 3 within 84 days.

The results shown in all Figures above (4-9) clarify the increase in soil penetration resistance when mixing soils with polymers for both PNS and POM. This increase, along with its further rise over time as the soil-polymer mixture hardens, can be explained by several factors. The findings demonstrated that soil penetration resistance increases over time when mixed with added polymers. This effect is attributed to several mechanisms. Polymers decrease porosity by binding fine soil particles and forming soil aggregates. These aggregates improve cohesion, leading to stronger interparticle contacts that require more force for penetration. Therefore, it is clear that physical hardening, caused by water evaporation in polymer-treated soil, continues over time. Additionally, chemical reactions through cross-linking between particles, along with physico-chemical interactions (e.g., cation exchange, hydrogen bonding), further stabilize the soil structure.

3.3 Regression Analysis Results and Predictive Equation

A multivariable linear regression analysis was used to model soil resistance as a function of curing time and polymer content for PNS- and POM-treated soils. For each site, 25 data points were collected from five curing times (1–28 days) and five polymer concentrations (10–50%). The fitted regression model, R=a + bT + cP, used R for soil resistance (kN/m²), T for curing time (days), and P for polymer content (%). Model performance was evaluated with R², RMSE, and MAE. Subsequently, site-specific models were combined by averaging the regression coefficients to create general predictive equations for each polymer type (PNS and POM).

3.3.1 PNS-treated soil Model:

The fit the linear model is $R = a + b\,T + c\,P$ where R is the penetration resistance (kN/m²), T is the curing time (days), P is the polymer content (%), a is the intercept, and b and c are regression coefficients associated with curing time and polymer content, respectively.

Table 3 the summary result of predictive equation factors and statistical parameters.

Site	a (Intercept)	B (per day)	C (slope: per 1% PNS)	R²	RMSE (kN/m²)	MAE (kN/m²)
Site#1	1.4126	0.2348	0.1773	0.9686	0.6077	0.5043
Site#2	1.4737	0.2275	0.1768	0.9692	0.5924	0.5194
Site#3	1.5352	0.2263	0.1733	0.9697	0.5799	0.4926

All three sites exhibit very strong linear predictability, with $R^2 = 0.97$ across the board. For the curing time effect, noted as (b), it is very consistent across the three sites (Site#1: 0.235, Site#2: 0.228, and Site#3: 0.226). This indicates that increasing curing time by 1 day raises resistance by approximately 0.23 kN/m², assuming PNS% remains constant. For the effect of polymer content, noted as (c), the PNS coefficient c is also consistent at the three sites (Site#1: 0.1773, Site#2: 0.1768, and Site#3: 0.1733). This shows that increasing PNS by 1% increases resistance by about 0.17–0.18 kN/m², while holding curing time constant. For the validity range, these equations are most reliable within the measured ranges, so that T = 1 to 28 days, and P = 10% to 50%, because the model is linear; extrapolating far beyond those ranges may reduce accuracy.

3.3.2 POM-treated Soil Model:

The fitted linear regression model is expressed as $R = a + b\,T + c\,P$, where T is curing time (days), P is POM additive content (%), and R is soil resistance (kN/m²).

Table 4 Summary results of model equation factors and statistical parameters.

Site	a (Intercept)	B (per day)	C (slope: per 1% POM)	R²	RMSE (kN/m²)	MAE (kN/m²)
Site#1	1.8014	0.2653	0.1854	0.9905	0.3592	0.2873
Site#2	1.589	0.2706	0.1851	0.9881	0.4047	0.3094
Site#3	1.4771	0.2684	0.1875	0.9856	0.4472	0.3666

Regarding overall model performance, the linear models fit very well across sites ($R^2 \approx 0.986–0.990$). Curing-time sensitivity remains consistent: b ≈ 0.265–0.271 kN/m² per day. POM-content sensitivity is also consistent: c ≈ 0.185–0.188 kN/m² per 1% POM. Prediction errors are relatively low for a simple linear model: RMSE ≈ 0.36–0.45 kN/m².

3.3.3 Comparison of PNS- and POM- treated soil Models:

The key comparative findings summarize that POM consistently outperforms PNS across all three sites. The Curing time sensitivity (b) is higher for POM at every site, which means faster strength gains with time. In addition, Polymer content sensitivity (c) is also higher for POM, which means greater benefit per 1% additive. Further, the prediction accuracy improves significantly with POM, where RMSE is reduced by ~30–40% compared to PNS. From an engineering perspective, this means that within the tested ranges, POM is more effective than PNS for enhancing soil resistance, both in the magnitude of strength gain and model reliability.

3.3.4 The General Predictive Equations:

Using the site-specific equations already derived for Sites #1, #2, and #3, simple arithmetic averages of the coefficients a, b, and c were done to obtain one general equation for PNS and one general equation for POM. For PNS-treated soil models, the averaged coefficients were computed, resulting in $\bar{a}_{pns}$, almost equal

to 1.474; $\bar{b}_{pns}$, nearly 0.2295; and $\bar{c}_{pns}$, about 0.1758. Therefore, the general PNS predictive equation is (Equation 1), which is graphically represented in Figure 10;

$R_{PNS} = 1.474 + 0.2295\,T + 0.1758\,P$ Eq. (1)

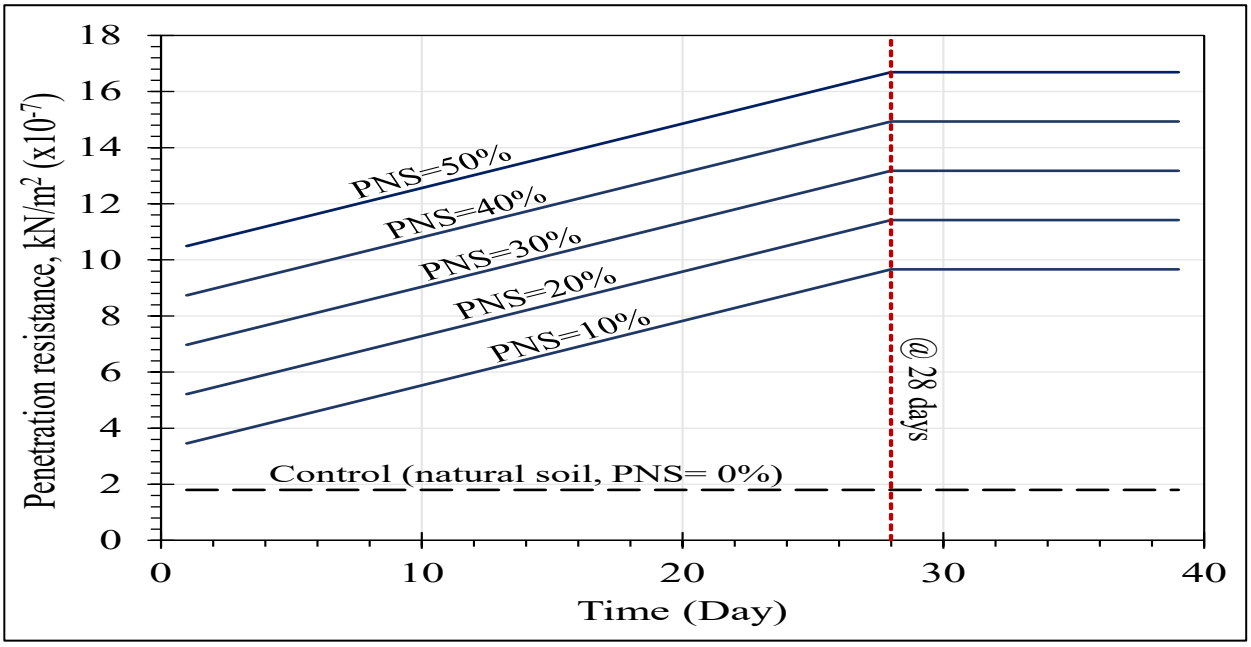

Figure 10: The general developed diagram of the PNS-treated soil model.

For PNS-treated soil models, the averaged coefficients were calculated, and the results show that $\bar{a}_{POM}$ is almost equal to 1.622, $\bar{b}_{POM}$ is nearly 0.2681, and $\bar{c}_{POM}$ is approximately 0.1860. So, the General PNS equation is given by Equation 2, which is graphically represented in Figure 11.

$R_{POM} = 1.622 + 0.2681\,T + 0.1860\,P$ Eq. (2)

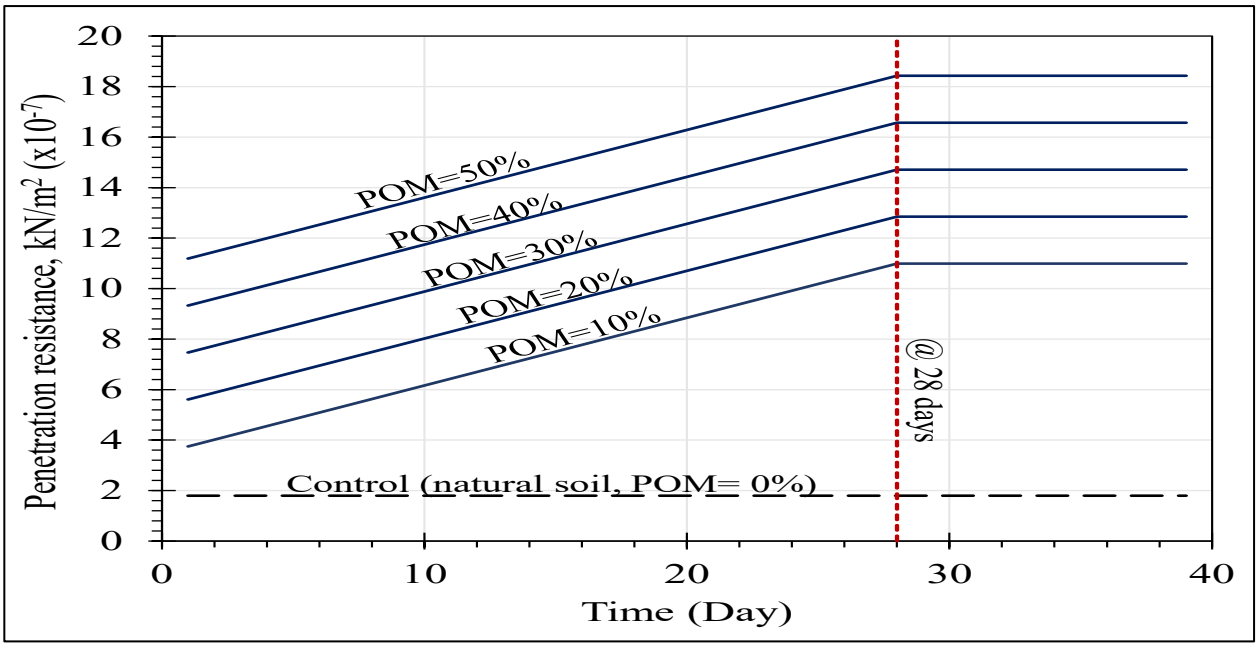

Figure 11: The general developed diagram of the POM- treated soil model

3.4 Results of Mineralogical Analysis

Table 5 presents the analysis results, which identify light minerals such as quartz and feldspar, as well as rock fragments. In contrast, Table 6 displays the primary heavy minerals in the sediment, including zircon, tourmaline, opaque minerals, pyroxene, epidote, chlorite, and biotite. Light minerals are mostly composed of quartz (monocrystalline ≈23.4–27.3%, polycrystalline ≈3.1–5.1%), feldspars, and carbonate rock fragments, along with contributions from chert, mudstone, igneous and metamorphic rock fragments, and

minor evaporites. Heavy minerals make up about 2.8–3.6% of the total sand and are mainly opaque minerals, chlorite, pyroxenes, mica (biotite, muscovite), hornblende, zircon, tourmaline, rutile, epidote, garnet, staurolite, and kyanite.

Table 5 Light Minerals Identified at Five Sites Using Polarized Microscopy.

Light Minerals		**Sample No.**				
		S1	**S2**	**S3**	**S4**	**S5**
Quartz	Monocrystalline Quartz	24.4	26.3	24.1	27.3	23.4
	Polycrystalline Quartz	3.1	4.4	3.6	5.1	4.2
Feldspars	Potash Feldspar	4.9	3.5	3.1	4.5	3.4
	Plagioclase Feldspar	4.4	3.6	4.6	5.2	4.7
Rock Fragments	Carbonate Rock Fragments	31.9	29.2	31.4	31.1	37.2
	Chert Rock Fragments	8.5	6.8	7.2	5.6	6.4
	Mudstone Rock Fragments	6.4	7.9	5.1	6.5	5.1
	Evaporites (Gypsum and Salts)	3.8	4.8	5.7	3.4	4.2
	Igneous Rock Fragment	5.3	5.5	6.2	5.7	5.2
	Metamorphic Rock Fragments	4.8	2.3	4.6	3.5	4.1
Coated Grains by Clay		1.2	2.1	2.5	0.9	1.2
Others		1.5	0.6	0.9	1.2	0.9

Table 6 shows that quartz makes up a large portion of the sample, which means the area has gone through long periods of weathering and erosion. The landscape likely used to be an ancient riverbed, nowadays dry and low in nutrients, with fast-draining soils. The small amount of granite and other igneous rocks supports this fact. Further, the presence of feldspar minerals indicates weathering processes of igneous rocks, such as granite.

Also, the soil shows a lot of calcium carbonate, which happens as a result of the weathering of limestone and dolomite rocks, increasing the calcium carbonate content. The findings point to a transition from a nutrient-rich environment to one experiencing dryness, over time.

In terms of soil resistance, quartz and carbonate fragments (29.2–37.2%) are the most influential light minerals. In quartz-rich dune soils, strength improvements after treatment are controlled primarily by polymer-induced bonding and surface crust formation, rather than by inherent mineral cementation (Garcia et al., 2015).

Table 6 Heavy minerals identified at five sites using polarized microscopy.

Heavy Minerals		**Samples No.**				
		S1	**S2**	**S3**	**S4**	**S5**
Opaques		35.3	36.8	35.4	36.5	35.9
Chlorite		6.4	7.2	8.2	7.3	8.5
Pyroxene Group	Orthopyroxene	2.6	2.3	2.3	2.7	2.2
	Clinipyroxene	4.5	5.4	4.1	4.4	4.5
Mica Group	Biotite	6.7	4.3	4.2	5.4	4.7
	Muscovite	4.8	5.1	5.5	5.2	4.4
Hornblende		5.1	6.8	5.7	6.5	7.4
Zircon		8.2	7.6	6.3	6.2	4.3
Tourmaline		7.3	6.7	7.1	6.7	8.2
Rutile		6.1	5.4	6.6	5.2	4.5
Epidote		5.9	4.3	4.5	6.1	4.9
Garnet		3.5	2.9	3.6	3.3	4.5
Staurolite		1.4	2.7	2.3	1.7	2.2
Kyanite		1.2	1.3	2.5	1.2	1.6
Others		0.9	1.2	1.5	0.6	1.2

Many diagnostic heavy-mineral species are very durable; for example, zircon (4.3-8.2) stays stable during mechanical and chemical weathering, rutile (4.5-6.6) is highly resistant to weathering, and tourmaline (6.7-8.2) is chemically and mechanically stable. This durability allows these minerals to survive multiple sedimentary cycles (Mohanty et al., 2023; Kotowski et al., 2021; Guo et al., 2021). Although Table 6 shows that opaque minerals, which come from mafic and ultramafic igneous rocks, are dominant, this study emphasizes non-opaque minerals such as Tourmaline, Staurolite, Rutile, Zircon, Apatite, and Kyanite. Gathering the stable heavy minerals (Tourmaline, Zircon, Rutile, and Garnet) indicates that the sediments are mineralogically mature.

4 Discussion

4.1 Mechanical Behaviour of Treated vs Untreated Dune Soils

The very low penetration resistance values of untreated dune soils are typical of quartz-dominated dune soil, where interparticle contacts are weak and resistance to penetration is mainly due to friction rather than bonding. This low-resistance behavior has been commonly reported in studies on dune stabilization and wind erosion control (Xing et al., 2018). In contrast, the treated soils showed a clear increase in penetration resistance as polymer concentration and curing time increased. This improvement is due to the cellulose-based dual-polymer curing agent adsorbing onto particles, forming a stabilizing layer and increasing strength with curing age (Yuan et al., 2020), thus causing reduction in voids and binding particles. While the penetration resistance of the treated soil consistently increased, reaching maximum values after 28 days and then remaining steady. After 28 days, resistance values stabilized and approached a quasi-equilibrium state regarding bonding and stiffness, similar to findings reported for biopolymer-treated sandy soils (Mohammadian et al., 2024).

For the regression analysis modeling, it revealed a strong, positive correlation among penetration resistance, polymer concentration, and curing time (developed diagrams of Figures 10 and 11). This robust relationship indicates the progressive strengthening of interparticle bonds and the formation of a more durable polymer network within the soil matrix. Additionally, the positive dependence on curing time reveals that resistance improvements are gradual rather than immediate, developing as the polymer structure stabilizes and moisture levels reach equilibrium. The consistent influence of two variables (polymer concentration and curing time) across different sites suggests that the treatment response is systematic and reproducible, not site-specific, where similar trends have been observed across various soils and polymers (Lemboye & Almajed, 2023).

4.2 Heavy-to-Light Mineral Ratio Effects

Table 7 presents the percentage-weight relationship between heavy and light minerals in the investigated dune sediments, expressed as the heavy-to-light mineral ratio. The results indicate that heavy minerals constitute a minor fraction of the total sediment mass, ranging from approximately 2.8 to 3.6%, corresponding to heavy-to-light ratios of 0.029 to 0.037%.

Table 7 Percentage weight of Heavy to Light minerals.

Sample No.	sample (gm)	Light Minerals (gm)	Light Minerals (%)	Heavy Minerals (gm)	Heavy Minerals (%)	Heavy to Light Minerals
S1	5	4.86	97.2	0.14	2.8	0.029
S2	5	4.85	97.0	0.15	3.0	0.031
S3	5	4.84	96.8	0.16	3.2	0.033
S4	5	4.86	97.2	0.14	2.8	0.029
S5	5	4.82	96.4	0.18	3.6	0.037

Such values, where light minerals form the structural framework of the studied sediment and heavy minerals occur only as accessory components. This limited proportion of heavy minerals implies that their direct contribution to bulk mechanical resistance is secondary compared with that of the light-mineral framework, particularly quartz and carbonate rock fragments. In untreated dune sediments, penetration resistance is thus expected to be controlled essentially based on packing density, grain size distribution, and particle shape rather than by the heavy-to-light mineral ratio itself. In the context of polymer-treated soils, the role of the heavy-to-light mineral ratio is further diminished, and the mechanical behaviour observed in treated samples is governed mainly by polymer-induced bonding and curing-time-dependent hardening processes.

5 Conclusions

This paper aimed to experimentally evaluate the effectiveness of carboxymethyl cellulose (CMC) polymer for stabilizing active dune sediments by testing five dune-soil samples collected from highway-adjacent dune fields, southern Iraq. The program combined chemical, physical, mineralogical, penetration resistance, and statistical regression analyses to develop predictive equations. It can be concluded:

- Chemical and physical characterization of the untreated soil are typical of quartz-dominated aeolian sands, (natural) dune soils showed high total porosity (52.1%), low bulk density (1.27 g cm^{-3}), low plasticity (PI ≈7.8), and moderately saline–alkaline conditions (EC =3.5 dS m^{-1}; pH =7.5), highlighted the high susceptibility to erosion and dune migration.
- Penetration resistance tests demonstrated a substantial and systematic increase in soil strength with increasing CMC content and curing time at all investigated sites.
- Regression modeling produced highly reliable predictive relationships (Equations 1 and 2) between penetration resistance, curing time, and polymer content. For PNS-treated soils, coefficients of determination were $R^2 \approx 0.97$, while POM-treated soils achieved $R^2 \approx 0.986–0.991$, confirming higher prediction accuracy and engineering reliability.
- Mineralogical analysis revealed a homogenous, quartz-dominated dune sediment, and a low heavy-mineral content of only 2.8–3.6%, corresponding to heavy-to-light mineral ratios of 0.029–0.037 in all samples. This mineralogical homogeneity confirms that observed strength improvements are controlled primarily by polymer bonding and curing processes rather than by inherent mineralogical variability.
- The CMC treatment provides a scalable, low-cost, and environmentally compatible solution for dune stabilization in southern Iraq. Lower polymer additives (around 10–20%) are suitable for dust suppression and land rehabilitation, while higher additives (40–50%) provide sufficient mechanical resistance for infrastructure-adjacent applications such as highways, service roads, and industrial zones exposed to active dune encroachment.

Acknowledgments
The authors acknowledge the University of Basrah, Iraq, for providing financial assistance and the Marine Science Center, Basra, Iraq, for providing the technical facilities during the research.

Funding Source
The authors declare that no funding was received during the preparation of this research.

Data Availability Statement
The data that support the findings of this study are available on request from the corresponding author.

Compliance with Ethical Standards
The authors declare that the results of the study did not involve human and/or animal rights.

Conflict of Interest
The authors declare that they have no conflict of interest.

References

1. Abdelgelil, A. A., Omer, A. M., Hassan, A. F., Moustafa, A. A., & Mohy Eldin, M. S. (2025b). Enhancement of sandy soil water retention using superabsorbent carboxymethyl cellulose grafted with polyacrylamide and poly(acrylamidomethyl propanesulfonic acid) copolymer. Scientific Reports, 15(1), Article 16604. https://doi.org/10.1038/s41598-025-16604
2. Abdelgelil, M., Omer, A. M., Hassan, A. F., Moustafa, A. A., & Mohy Eldin, M. S. (2025a). Microstructural analysis of NaCMC-stabilized clay soils. Geotechnical Testing Journal, 48(2), 345–362.
3. Amézketa, E. (1999). Soil aggregate stability: A review. Journal of Sustainable Agriculture, 14(2–3), 83–151. https://doi.org/10.1300/J064v14n02_08
4. Chang, I., Im, J., Prasidhi, A. K., & Cho, G. C. (2020). Biopolymer-based soil treatment for dust control. Construction and Building Materials, 242, Article 118091.
https://doi.org/10.1016/j.conbuildmat.2020.118091

5. Chen, R., Zhang, L., Liu, X., & Yang, Y. (2019). Crust formation mechanisms in polymer-stabilized sands. Geoderma, 353, 118–127. https://doi.org/10.1016/j.geoderma.2019.06.028
6. Colip, G. D., Chirico, P., Lair, A., & Seidenstein, J. L. (2025). Multi-proxy geochemical and sedimentological data from 20 short sediment cores collected along the Euphrates, Tigris, and Shatt al-Gharraf rivers in the lower Mesopotamian Plain, Iraq. U.S. Geological Survey Data Release. https://doi.org/10.5066/P13HGVV2
7. Garcia, N. F., Valdes, J. R., & Cortes, D. D. (2015). Strength characteristics of polymer-bonded sands. Géotechnique Letters, 5(3), 212–216.
8. Guo, R., Hua, X., Garzanti, E., & Lai, W. (2021). Boron isotope composition of detrital tourmaline: A new tool in provenance analysis. Lithos, 400–401, Article 106360.
https://doi.org/10.1016/j.lithos.2021.106360
9. IPCC (Intergovernmental Panel on Climate Change). (2019). Climate change and land: An IPCC special report on climate change, desertification, land degradation, sustainable land management, food security, and greenhouse gas fluxes in terrestrial ecosystems.
10.Iraq I.O.M. (International Organization for Migration). (2022). Migration, environment, and climate change in Iraq.
11.Kotowski, J., Nejbert, K., & Olszewska-Nejbert, D. (2021). Rutile mineral chemistry and Zr-in-rutile thermometry in provenance studies. Minerals, 11(6), Article 553. https://doi.org/10.3390/min11060553
12.Lemboye, K., & Almajed, A. (2023). Effect of varying curing conditions on the strength of biopolymer-modified sand. Polymers, 15(7), Article 1678. https://doi.org/10.3390/polym15071678
13.Mirzabaev, A., Stringer, L. C., Benjaminsen, T. A., Gonzalez, P., Harris, R., Jafari, M., Stevens, N., Tirado, C. M., & Zakieldeen, S. (2022). Deserts, semiarid areas and desertification. In H.-O. Pörtner et al. (Eds.), Climate change 2022: Impacts, adaptation and vulnerability (pp. 2195–2231). Cambridge University Press. https://doi.org/10.1017/9781009325844.020
14.Mirzaei, M., Zare, S., & Khosravi, H. (2021). Wind tunnel evaluation of biopolymer erosion control. Aeolian Research, 50, Article 100679. https://doi.org/10.1016/j.aeolia.2021.100679
15.Mohammadian, F., Abdolsamadi Bonab, B., & Oliaei, M. (2024). A comprehensive review of biodegradable biopolymers' challenges and performance in improving soil mechanical characteristics. Environmental Earth Sciences, 83, Article 680. https://doi.org/10.1007/s12665-024-11891-w.
16.Mohanty, S., Papadopoulos, A., Petrelli, M., Papadopoulou, L., & Sengupta, D. (2023). Geochemical studies of detrital zircon grains from river banks and beach placers. Minerals, 13(2), Article 192. https://doi.org/10.3390/min13020192.
17.Othman, A. A., Al-Saady, Y. I., Shihab, A. T., & Al-Maamar, A. F. (2019). The aeolian sand dunes in Iraq: A new insight. In Environmental remote sensing and GIS in Iraq (pp. 279–300). Springer. https://doi.org/10.1007/978-3-030-21344-2_12.
18.Rammal, M. M., & Jubair, A. A. (2015). Sand dune stabilization using silica gel and cement kiln dust. Nahrain University College of Engineering Journal, 18(2), 179–191.
19.Sissakian, V. K., & Fouad, S. F. (2015). Geological map of Iraq, scale 1:1,000,000 (2012). Iraqi Bulletin of Geology and Mining, 11(1), 9–16.
20.Sissakian, V. K., Al-Ansari, N., & Adamo, N. (2021). Geomorphology, stratigraphy and tectonics of the Mesopotamian Plain, Iraq: A critical review. Geotectonics, 55(1), 135–160.
https://doi.org/10.1134/S001685212101012X.
21.Soils and Foundations, 60(4), 1023–1034. https://doi.org/10.1016/j.sandf.2020.05.011.
22.Soldo, A., Miletić, M., & Jug, D. (2020). Moisture retention in biopolymer-treated soils.
23.Sujatha, A., & Kannan, R. (2022a). Advances in sand dune stabilization techniques. Journal of Geotechnical Engineering.
24.Sujatha, E. R., & Kannan, G. (2022b). An investigation on the potential of cellulose for soil stabilization. Sustainability, 14(23), Article 16277. https://doi.org/10.3390/su142316277.
25.UNCCD (United Nations Convention to Combat Desertification). (2019). Creating an enabling environment for land degradation neutrality and its potential contribution to enhancing well-being, livelihoods and the environment. UNCCD Secretariat.
26.UNCCD (United Nations Convention to Combat Desertification). (2018). Desertification. https://www.unccd.int/land-and-life/desertification/overview.
27.Xing, C., Liu, X., & Anupam, K. (2018). Response of sandy soil stabilized by polymer additives. Open Access Journal of Environmental and Soil Sciences, 1, 1–8.

28.Yahia, M. M. M., Muttashar, W. R., Shbaar, H. A., & Haddad, A. M. (2023). Improving the mechanical properties of dune soils in southern Iraq by adding carboxymethyl cellulose. IOP Conference Series: Earth and Environmental Science, 1215(1), Article 012026.
29.Yuan, J., Ye, C., Luo, L., Pei, X., Yang, Q., Chen, J., & Liao, B. (2020). Sand fixation property and erosion control through new cellulose-based curing agent on sandy slopes under rainfall. Bulletin of Engineering Geology and the Environment, 79, 4051–4061. https://doi.org/10.1007/s10064-020-01807-w.
30.Zhang, Z., Li, Z., Yao, L., Chang, S., & Wu, Y. (2024). Development and performance evaluation of sunflower straw cellulose ether ecological sand-fixing material. BioResources, 19(2), 2201–2215.